JOURNAL OF PHYSICAL ORGANIC CHEMISTRY
J. Phys. Org. Chem. 2001; **14:** 644–649
DOI:10.1002/poc.403

A quantum-chemical study of PBX: intermolecular interactions of TATB with CH_2F_2 and with linear fluorine-containing polymers

He-Ming Xiao,[1]* Jin-Shan Li[1,2] and Hai-Shan Dong[2]

[1]Department of Chemistry, Nanjing University of Science and Technology, Nanjing 210094, People's Republic of China
[2]Institute of Chemical Materials, China Academy of Engineering Physics, Mianyang 621900, People's Republic of China

Received 12 October 1999; revised 9 February 2000; accepted 27 April 2000

ABSTRACT: The calculations of density functional theory at the B3LYP/3-21G* level have been employed to optimize the 1,3,5-triamino-2,4,6-trinitrobenzene (TATB)$\cdots CH_2F_2$ complex. The complex binding energy is corrected for the basis set superposition error. In addition, the interactions of TATB with $-(-CUV—CXY-)_{\overline{n}}$ (U, V, X, Y = H. U = F; V, X, Y = H. U, V = F; X, Y = H. U, V, X = F; Y = H. U, V, X, Y = F. U, V, X = F; Y = Cl) have been studied with the MO-PM3 method, and the complex binding energy with approximation of electron correlation correction by the dispersion energy has been given. The results computed indicate that the greatest corrected binding energy of TATB and CH_2F_2 is $-4.62\ kJ\ mol^{-1}$ at the B3LYP/6-311G*//B3LYP/3-21G* level. The interactions of $-(-CF_2—CH_2-)_{\overline{n}}$ with TATB and of $-(-CF_2—CFH-)_{\overline{n}}$ with TATB are stronger than those of $-(-CUV—CXY-)_{\overline{n}}$ (U, V, X, Y = H. U = F; V, X, Y = H. U, V, X, Y = F. U, V, X = F; Y = Cl) with TATB ($n = 5$). Copyright © 2001 John Wiley & Sons, Ltd.

KEYWORDS: 1,3,5-triamino-2,4,6-trinitrobenzene; fluorine-containing polymer; intermolecular interaction; DFT-B3LYP method; MO-PM3 method

INTRODUCTION

Since the first formulation of polymer-bonded explosive (PBX-9205) in 1947, the PBXs have been widely used in many fields, such as missiles, aviation, mineral exploration, etc.[1–4] One of the key techniques of PBX development is how to acquire polymers that have a strong interaction with the pure explosive. In general, the interactions among the PBX components are determined experimentally by the measurements of mechanical properties, interface properties, etc.,[4,5] and are explained using acid–base theory, diffusion theory, and interfacial theory.[6,7] However, these theories are dependent on experiments or are qualitative.

In the last several decades, important progress in the investigation of intermolecular interactions using quantum-chemical methods has been made.[8–14] The intermolecular interaction plays a significant role in the development of PBX formulations,[4,5,15] and, in view of this, molecular dynamical and quantum-chemical methods have recently been employed to investigate the interactions.[16–18]

So far 1,3,5-triamino-2,4,6-trinitrobenzene (TATB) has been the sole pure insensitive high explosive.[19] The research of TATB-based PBXs is important to satisfy the demands of safety. Usually, fluorine-containing polymers are used to bond TATB[1,2] because they have the advantages of large density, good stability, and so forth. Although there are some studies on the intermolecular interaction of fluorine-containing systems,[20,21] no quantum-chemical investigation on the interaction between TATB and fluorine-containing polymers has been reported. In this paper we employ the B3LYP[22] and MO-PM3[23] methods to study the TATB$\cdots CH_2F_2$ complex and the TATB$\cdots$ $-(-CUV—CXY-)_{\overline{n}}$ (U, V, X, Y = H. U = F; V, X, Y = H. U, V = F; X, Y = H. U, V, X = F; Y = H. U, V, X, Y = F. U, V, X = F; Y = Cl) complexes respectively. Optimized geometries, electronic structures, and binding energies have been obtained. Additionally, we have tried to shed some light on the design of PBX formulations.

**Correspondence to:* J. Xiao, Department of Chemistry, Nanjing University of Science and Technology, Nanjing 210094, People's Republic of China.

COMPUTATIONAL METHODS

Geometrical optimizations and electronic structural calculations

The full geometry optimizations of TATB and of CH_2F_2 are performed at the B3LYP/3-21G* level. Since the full

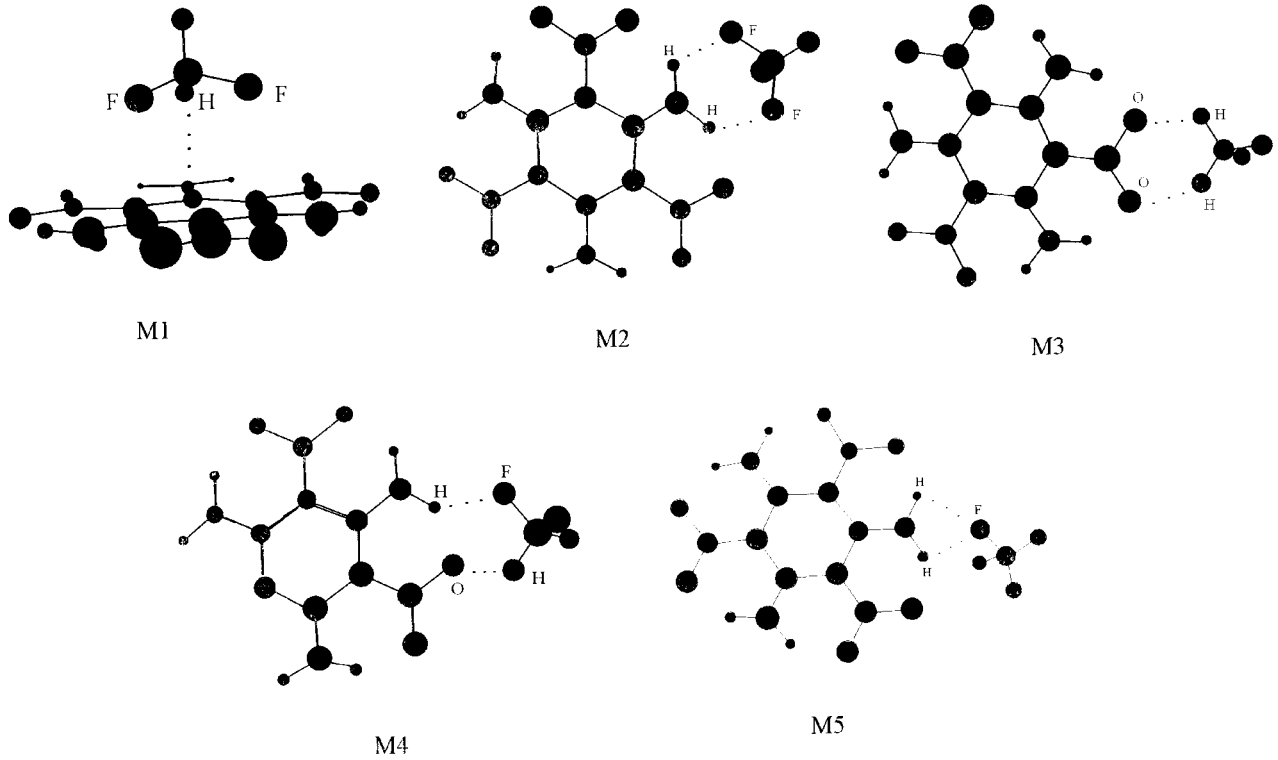

Figure 1. The structures of TATB + CH_2F_2 created by the Chem3D software

geometry optimizations of the TATB···CH_2F_2 complex are expensive, in this paper we treat TATB and CH_2F_2 with rigid model.[24] The intermolecular coordinates of the possible stable structures of the TATB···CH_2F_2 complex acquired with Chem3D software,[25] which are shown in Fig. 1, are optimized at the B3LYP/3-21G* level. For the TATB···$\{$CUV—CXY$\}_n$ systems we adopt the semi-empirical MO-PM3 method. All the MO-PM3 calculations for the TATB···$\{$CUV—CXY$\}_n$ complexes are performed on the possible stable structures created by the Chem3D software (for brevity, the complex structures created are not given). The end groups of linear $\{$CUV—CXY$\}_n$ are considered as H atoms, and the chain grows in head-to-tail orientation. Natural bond orbital analyses[26] on the optimized structures of the TATB···CH_2F_2 complex are carried out at the B3LYP/3-21G* level.

Calculation of intermolecular interaction energy

The intermolecular interaction energy ΔE of the complex is evaluated as the sum of the self-consistent field (SCF) interaction energy ΔE^{SCF} and the correlation interaction energy ΔE^{COR}.[24] For the B3LYP calculations, ΔE is determined as the difference between the total energy of the complex and the sum of the total energies of the isolated molecules, and is corrected for basis set superposition error (BSSE)[27] with the Boys–Bernardi method.[8] For the MO-PM3 calculation, ΔE^{SCF} is calculated by ΔE^{PM3}, and ΔE^{COR} is approximated by the dispersion energy ΔE^{D}.[28] Then the intermolecular interaction energy of the complex is evaluated approximately as

$$\Delta E = \Delta E^{PM3} + \Delta E^{D} \quad (1)$$

$$\Delta E^{D} = -\sum_{i}^{A}\sum_{j}^{B} C_{ij} R_{ij}^{-6} \quad (2)$$

Summation over i and j is carried out over all the atoms of subsystems A and B; r_{ij} is the distance between atoms i and j, C_{ij} is a coefficient equal to the geometrical mean of C_{ii} and C_{jj}. The values of C_{ii} (kJ mol Å^{-6}) for C, H, N, O, F and Cl are 2254.2, 103.8, 1510.5, 882.1, 511.4 and 7033.5 respectively.[24]

All calculations were carried out with the Gaussian 94 program[29] implemented on a PII personal computer using the default Gaussian convergence criteria.

RESULTS AND DISCUSSIONS

Interaction of TATB with CH_2F_2

Table 1 gives the fully optimized geometrical parameters of TATB and of CH_2F_2 at the B3LYP/3-21G* level. From Table 1 we can see that TATB is practically a planar molecule. At the B3LYP/3-21G* level we obtain three optimized structures (I–III, see Fig. 2) for the

Table 1. The fully optimized geometrical parameters of TATB and of CH_2F_2 at the B3LYP/3-21G* level (bond length r/nm; dihedral angle θ/degrees)

TATB molecule				CH_2F_2 molecule
$r_{2-1} = 0.1441$	$\theta_{13-7-1-2} = -0.06$	$\theta_{18-11-5-6} = 0.00$	$\theta_{23-12-6-1} = 0.02$	$r_{2-1} = 0.1392$
$r_{7-1} = 0.1323$	$\theta_{14-7-1-2} = 179.97$	$\theta_{19-8-2-1} = 0.13$	$\theta_{24-12-6-1} = -179.99$	$r_{4-1} = 0.1094$
$r_{8-2} = 0.1416$	$\theta_{15-9-3-4} = 179.96$	$\theta_{20-8-2-1} = -179.88$		$\theta_{4-1-2-3} = -119.39$
$r_{13-7} = 0.1033$	$\theta_{16-9-3-4} = -0.02$	$\theta_{21-10-4-3} = 0.02$		$\theta_{5-1-2-3} = 119.39$
$r_{19-8} = 0.1314$	$\theta_{17-11-5-6} = 180.00$	$\theta_{22-10-4-3} = -179.98$		

$TATB\cdots CH_2F_2$ complex (structures M1, M4 and M5 converge on I, and M2 and M3 converge on II and III respectively).

Table 2 lists the calculated total energy E and the intermolecular interaction energy by the B3LYP method with 3-21G*, 4-31G*, 6-31G* and 6-311G* basis sets, where ΔE_C is the ΔE corrected for the BSSE. By comparing ΔE_C with ΔE (see Table 2) we find that the smaller the basis set, the larger is the BSSE; hence the BSSE correction is important to the accurate calculation of the complex binding energy with the B3LYP method. For structures I, II and III the values of $-\Delta E_C$ are in the order I $\approx$ III $>$II at the B3LYP/3-21G* level, are very close at the B3LYP/4-31G*//B3LYP/3-21G* level, and are in the order I $>$ III $>$ II at both the B3LYP/6-31G*//B3LYP/3-21G* and the B3LYP/6-311G*//B3LYP/3-21G* levels. At the B3LYP/6-311G*//B3LYP/3-21G* level the greatest corrected binding energy of TATB and CH_2F_2 is -4.62 kJ mol^{-1}.

The values of charge transfer from TATB to CH_2F_2 are $-0.015e$, $-0.038e$ and $0.028e$ for structures I, II and III respectively from the natural bond orbital (NBO) analysis. The calculated occupancies of NBOs at the B3LYP/3-21G* level are displayed in Table 3. Compared with the isolated TATB and the isolated CH_2F_2, for structure I the occupancy of the N(9)—H(16) antibond increases by 0.014 (see Table 3), the occupancy of lone pair (2) of the F(3) atom decreases by 0.014, and the occupancies of other NBOs have smaller changes. Considering the optimized structure I, it can be concluded that the charge transfer between subsystems in I arises chiefly between the N(9)—H(16) antibond and the lone pair of the F(3) atom. Similar analyses show that there exists in II a charge transfer between the N(11)—H(18) antibond and the lone pair of the F(2) atom and between the N(11)—H(17) antibond and the F(3) lone pair, and in III chiefly between the O(19) lone pair and the C(1)—H(5) antibond.

Interactions of TATB with $-(-CUV—CXY-)_n$

Interactions of TATB with $-(-CF_2—CH_2-)_n$ (n = 1, 2, 3, 4, 5).

$-(-CF_2—CH_2-)_n$ is a polymer. It is difficult to calculate the interaction between TATB and a polymer with quantum-chemical methods at present. Thus we

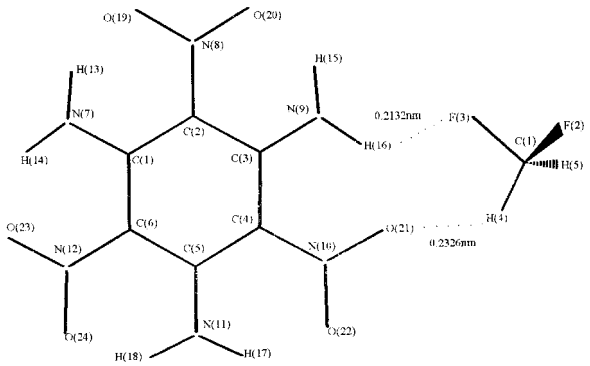

I

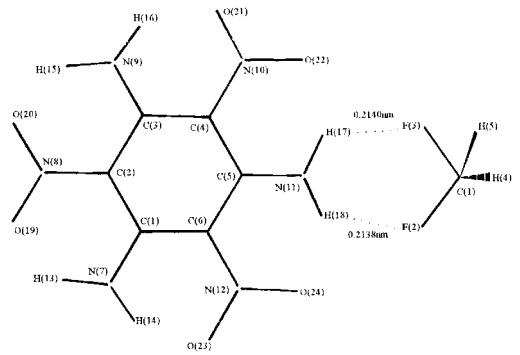

II

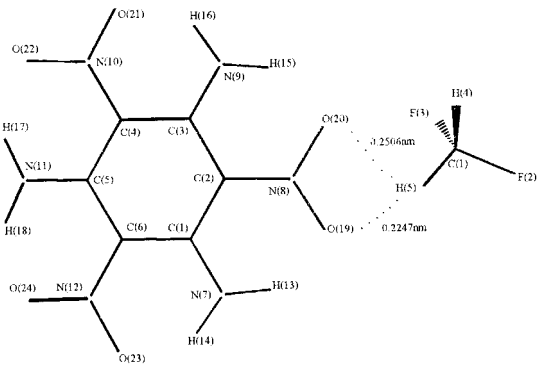

III

Figure 2. The optimized structures of the TATB and CH_2F_2 complex

Table 2. Total energies, intermolecular interaction energies and dipole moments (1 hartree = 2625.50 kJ mol^{-1})

Level		E (kJ mol^{-1})	ΔE (kJ mol^{-1})	ΔE_C (kJ mol^{-1})	Dipole moment (D)
B3LYP/3-21G*	TATB	−2641826.80			0.00
	CH_2F_2	−624007.42			1.94
	I	−3265871.79	−37.57	−4.53	1.90
	II	−3265872.09	−37.87	−1.98	3.34
	III	−3265864.92	−30.70	−4.59	3.04
B3LYP/4-31G*//B3LYP/3-21G*	I	−3280816.94	−18.95	−2.82	1.82
	II	−3280815.97	−17.98	−2.83	3.13
	III	−3280811.16	−13.18	−2.72	2.76
B3LYP/6-31G*//B3LYP/3-21G*	I	−3283934.94	−16.43	−3.23	1.83
	II	−3283932.94	−14.43	−2.63	3.12
	III	−3283929.50	−10.98	−2.85	2.74
B3LYP/6-311G*//B3LYP/3-21G*	I	−3284804.73	−14.72	−4.62	1.95
	II	−3284797.53	−7.52	−3.46	3.24
	III	−3284801.77	−11.76	−4.28	2.95

have to choose a model to simulate the linear polymer. Selecting this kind of model is possible and reliable because the chemical intuition and the calculated result tell us that the binding energy remains nearly unchanged while n increases to a certain number. We adopt a binding energy gap of 3 kJ mol^{-1} between the adjacent n as our

Table 3. Occupancies of selected NBOs at the B3LYP/3-21G* level

	Occupancy					Occupancy			
TATB NBO	Isolated	I	II	III	CH_2F_2NBO	Isolated	I	II	III
C(2)—N(8) bond	1.727	1.727	1.731	1.738	C(1)—F(2) bond	1.996	1.996	1.995	1.996
C(3)—N(9) bond	1.963	1.961	1.964	1.963	C(1)—F(3) bond	1.996	1.995	1.995	1.996
C(4)—N(10) bond	1.727	1.735	1.728	–	C(1)—H(4) bond	1.996	1.995	1.996	1.996
C(5)—N(11) bond	1.963	1.963	1.961	1.963	C(1)—H(5) bond	1.996	1.995	1.996	1.996
N(8)—O(19) bond	1.994	1.994	1.994	1.993	F(2) lone pair(1)	1.994	1.994	1.988	1.994
N(8)—O(20) bond	1.994	1.994	1.994	1.994	F(2) lone pair(2)	1.966	1.968	1.968	1.968
N(9)—H(15) bond	1.987	1.986	1.987	1.987	F(2) lone pair(3)	1.918	1.917	1.912	1.919
N(9)—H(16) bond	1.987	1.986	1.987	1.987	F(3) lone pair(1)	1.994	1.990	1.988	1.994
N(10)—O(21) bond	1.994	1.994	1.994	1.994	F(3) lone pair(2)	1.966	1.952	1.968	1.968
N(10)—O(22) bond	1.994	1.994	1.994	1.994	F(3) lone pair(3)	1.918	1.923	1.912	1.920
N(11)—H(17) bond	1.987	1.987	1.986	1.987	C(1)—F(2) antibond	0.072	0.068	0.070	0.076
N(11)—H(18) bond	1.987	1.987	1.986	1.987	C(1)—F(3) antibond	0.072	0.075	0.070	0.073
O(19) lone pair(1)	1.973	1.973	1.973	1.964	C(1)—H(4) antibond	0.039	0.042	0.037	0.040
O(19) lone pair(2)	1.854	1.854	1.854	1.853	C(1)—H(5) antibond	0.039	0.038	0.037	0.050
O(20) lone pair(1)	1.973	1.973	1.973	1.969					
O(20) lone pair(2)	1.854	1.855	1.854	1.855					
O(21) lone pair(1)	1.973	1.966	1.973	1.973					
O(21) lone pair(2)	1.854	1.859	1.854	1.854					
O(22) lone pair(1)	1.973	1.973	1.973	1.973					
O(22) lone pair(2)	1.854	1.854	1.855	1.854					
C(2)—N(8) antibond	0.779	0.779	0.776	0.761					
C(3)—C(4) antibond	0.027	0.027	0.027	0.026					
C(3)—N(9) antibond	0.459	0.445	0.462	0.455					
C(4)—N(10) antibond	0.779	0.768	0.779	–					
C(5)—N(11) antibond	0.459	0.459	0.445	0.455					
N(8)—O(19) antibond	0.058	0.058	0.058	0.059					
N(8)—O(20) antibond	0.058	0.058	0.058	0.057					
N(9)—H(15) antibond	0.089	0.088	0.089	0.086					
N(9)—H(16) antibond	0.089	0.103	0.090	0.089					
N(10)—O(21) antibond	0.058	0.061	0.059	0.058					
N(10)—O(22) antibond	0.058	0.058	0.057	0.058					
N(11)—H(17) antibond	0.089	0.089	0.101	0.089					
N(11)—H(18) antibond	0.089	0.089	0.101	0.089					

Table 4. Total energies E^{PM3}, intermolecular interaction energies, and dipole moments for TATB and $-(-CF_2—CH_2-)_n$ (n = 1, 2, 3, 4, 5) calculated at the PM3 level (1 hartree = 2625.50 kJ mol^{-1})

Structures	E^{PM3} (kJ mol^{-1})	ΔE^{PM3} (kJ mol^{-1})	ΔE^{D} (kJ mol^{-1})	ΔE (kJ mol^{-1})	Dipole moment (D)
TATB	−45.23				0.07
1,1-Difluorineethane (n = 1)	−468.51				0.83
1,1,3,3-Tetrafluorinebutane (n = 2)	−911.76				1.61
1,1,3,3,5,5-Hexafluorinehexane (n = 3)	−1352.88				2.28
1,1,3,3,5,5,7,7-Octafluorineoctane (n = 4)	−1790.69				3.18
1,1,3,3,5,5,7,7,9,9-Decafluorinedecane (n = 5)	−2232.18				3.81
TATB + 1,1-difluorineethane	−523.20	−9.46	−10.75	−20.21	0.88
TATB + 1,1,3,3-tetrafluorinebutane	−971.32	−14.33	−15.32	−29.65	1.55
TATB + 1,1,3,3,5,5-hexafluorinehexane	−1416.42	−18.31	−18.70	−37.01	2.23
TATB + 1,1,3,3,5,5,7,7-octafluorineoctane	−1860.56	−24.64	−26.15	−50.79	3.02
TATB + 1,1,3,3,5,5,7,7,9,9-decafluorinedecane	−2302.97	−25.56	−27.42	−52.98	3.76

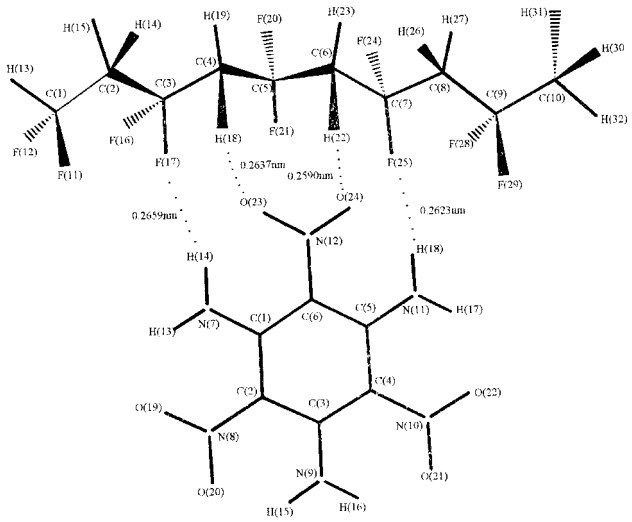

IV

Figure 3. The optimized structure of the TATB···1,1,3,3,5,5,7,7,9,9-decafluorinedecane complex

criterion for choosing the model. Table 4 lists the binding energy for n = 1 to 5. A look at Table 4 demonstrates that the binding energy of TATB with $-(-CF_2—CH_2-)_n$ increases gradually while n increases from 1 to 5; in particular, the $-\Delta E$ of 1,1,3,3,5,5,7,7,9,9-decafluorinedecane (n = 5) and TATB is 2.19 kJ mol^{-1} greater than that of 1,1,3,3,5,5,7,7-octafluorineoctane (n = 4) and TATB. So we shall select n = 5 for the following calculations. In addition, for every complex in Table 4 ΔE^{D} is close to ΔE^{PM3} (e.g. the value of $\Delta E^{D}/\Delta E^{PM3}$ for the TATB···decafluorinedecane complex is 1.07), indicating that the estimation of dispersion energy is necessary for the PM3 calculation.

The optimized structure of the TATB···decafluorinedecane complex is shown in Fig. 3. Table 5 reports the selected fully optimized geometrical parameters. By comparing the bond lengths of a single TATB molecule optimized by the B3LYP method with those by the PM3 method (see Tables 1 and 4), we find that the difference in N—O bond length between the B3LYP method (0.1314 nm) and the PM3 method (0.1226 nm) is 0.0088 nm and those of the other bond lengths are smaller. Compared with the isolated TATB and the isolated decafluorinedecane, for the TATB subsystem in IV, both the $r_{23–12}$ and the $r_{24–12}$ increase by 0.4 pm, the $r_{12–6}$ decreases by 1.7 pm; but all bond

Table 5. Selected fully optimized bond lengths (nm) by the PM3 method

	Decafluorinedecane			TATB	
Parameter	Isolated	IV	Parameter	Isolated	IV
$r_{4–3}$	0.1555	0.1553	$r_{6–5}$	0.1437	0.1439
$r_{5–4}$	0.1555	0.1554	$r_{7–1}$	0.1360	0.1355
$r_{6–5}$	0.1555	0.1554	$r_{11–5}$	0.1361	0.1354
$r_{7–6}$	0.1555	0.1552	$r_{12–6}$	0.1457	0.1440
$r_{17–3}$	0.1361	0.1362	$r_{13–7}$	0.1003	0.1002
$r_{18–4}$	0.1107	0.1109	$r_{14–7}$	0.1003	0.1003
$r_{20–5}$	0.1362	0.1362	$r_{17–11}$	0.1003	0.1002
$r_{21–5}$	0.1358	0.1360	$r_{18–11}$	0.1003	0.1003
$r_{22–6}$	0.1107	0.1109	$r_{23–12}$	0.1226	0.1230
$r_{23–6}$	0.1106	0.1106	$r_{24–12}$	0.1226	0.1230
$r_{29–9}$	0.1363	0.1366			

Table 6. Total energies E^{PM3}, intermolecular interaction energies and dipole moments for TATB and $-(-CUV—CXY-)_{\overline{n}}$ ($n = 5$) calculated at the PM3 level (1 hartree = 2625.50 kJ mol^{-1})

Structures	E^{PM3} (kJ mol^{-1})	ΔE^{PM3} (kJ mol^{-1})	ΔE^{D} (kJ mol^{-1})	ΔE (kJ mol^{-1})	Dipole moment (D)
U = H, V = H, X = H, Y = H (A)	−258.41				0.00
U = F, V = H, X = H, Y = H (B)	−1141.69				2.98
U = F, V = F, X = F, Y = H (C)	−3052.31				2.63
U = F, V = F, X = F, Y = F (D)	−4085.25				1.00
U = F, V = F, X = F, Y = Cl (E)	−3060.81				1.61
TATB + A	−311.71	−8.07	−28.20	−36.27	0.10
TATB + B	−1206.21	−19.29	−19.13	−38.42	3.20
TATB + C	−3123.89	−26.34	−22.12	−48.46	2.15
TATB + D	−4144.84	−14.36	−19.15	−33.51	1.17
TATB + E	−3118.89	−12.85	−15.54	−28.39	1.47

lengths of the decafluorinedecane subsystem do not change sharply.

Interactions of TATB with $-(-CUV—CXY-)_{\overline{n}}$ ($n = 5$). Table 6 displays the total energies E^{PM3}, intermolecular interaction energies and dipole moments for TATB and $-(-CUV—CXY-)_{\overline{n}}$ ($n = 5$) calculated by the PM3 method. From Tables 4 and 6, one can see that the binding energy of TATB with a linear fluorine-containing polymer does not increase with increasing numbers of F atoms in the polymer chain. The $-\Delta E$ values of $-(-CF_2—CH_2-)_{\overline{n}}$ with TATB and of $-(-CF_2—CFH-)_{\overline{n}}$ with TATB are larger than the others, whereas that of $(CF_2—CFCl)_n$ with TATB is the smallest; this demonstrates that the interactions between $-(-CF_2—CH_2-)_{\overline{n}}$ and TATB and between $-(-CF_2—CFH-)_{\overline{n}}$ and TATB are stronger. Therefore, in the development of TATB-based PBXs, one should pay attention to $-(-CF_2—CH_2-)_{\overline{n}}$ and $-(-CF_2—CFH-)_{\overline{n}}$.

CONCLUSIONS

The following conclusions are obtained from our theoretical investigations. (1) The interaction of an explosive molecule with a polymer chain in PBX can theoretically be simulated with quantum-chemical methods. (2) Three optimized structures of the TATB$\cdots CH_2F_2$ complex are obtained at the B3LYP/3-21G* level, whose greatest corrected binding energy is −4.62 kJ mol^{-1} at the B3LYP/6-311G*//B3LYP/3-21G* level. (3) The polymers $-(-CF_2—CH_2-)_{\overline{n}}$ and $-(-CF_2—CFH-)_{\overline{n}}$ should be examined in the preparation of TATB-based PBX.

REFERENCES

1. Dobratz BM, Crawford PC. *LLNL Explosives Handbook—Properties of Chemical Explosives and Explosive Simulants*. Lawrence Livermore National Laboratory, 1985; *UCRL*-52997.
2. Gibbs TR, Popolato A. *LASL High Explosives Property Data*. University of California Press, 1980.
3. Hoffman DM, Caley LE. *Polym. Eng. Sci.* 1986; **26**: 1489.
4. Sun G-X. *Polymer Mixed Explosives*. National Defense Industry Press: Beijing, 1984 (in Chinese).
5. Balley A, Bellerby JM, Kinloch SA. *Philos. Trans. R. Soc. London Ser. A* 1992; **339**: 321.
6. Van Oss CJ, Chaudhury MK, Good RJ. *Chem. Rev.* 1988; **88**: 927.
7. Xu QL. *Energ. Mater.* 1993; **1**: 1 (in Chinese).
8. Boys SF, Bernadi F. *Mol. Phys.* 1970; **19**: 553.
9. Mayer I. *Int. J. Quantum Chem.* 1983; **23**: 341.
10. Reed AE, Curtiss LA, Weinhold F. *Chem. Rev.* 1988; **88**: 899.
11. Mayer I, Vibok A, Valiron P. *Chem. Phys. Lett.* 1994; **224**: 166.
12. Paizs B, Suhai S. *J. Comp. Chem.* 1997; **18**: 694.
13. Hobza P. *Annu. Rep. Prog. Chem. Sect. C Phys. Chem.* 1997; **93**: 257.
14. Paizs B, Suhai S. *J. Comp. Chem.* 1998; **19**: 575.
15. Dong R, Xiao L, Jian D. *Explos. Shock Waves* 1995; **15**: 116 (in Chinese).
16. Cumming AS, Leiper GA, Robson E. *24th International Annual Conference of ICT*, Karlsruhe, Germany, 1993.
17. Li JS, Xiao HM, Dong HS. *Propell. Explos. Pyrotech.* 2000; **25**: 26.
18. Xiao HM, Li JS, Dong HS. *Acta Chim. Sinica* 2000; **58**: in press.
19. Graboske H. *Sci. Technol. Rev.* 1993; 3.
20. Waltman RJ. *J. Fluorine Chem.* 1998; **90**: 9.
21. Howard JAK, Hoy VJ, O'Hagan D, Smith GT. *Tetrahedron* 1996; **52**: 126163.
22. Becke AD. *J. Chem. Phys.* 1993; **98**: 5648.
23. Stewart JJP. *J. Comp. Chem.* 1989; **10**: 209.
24. Hobza P, Zahradnik R. *Chem. Rev.* 1988; **88**: 871.
25. CS Chem3D Pro™, Version 3.5, CambridgeSoft, Cambridge, MA, 1996.
26. Reed AE, Weinhold F. *J. Chem. Phys.* 1983; **78**: 4066.
27. Ransil BJ. *J. Chem. Phys.* 1961; **34**: 2109.
28. Hobza P, Sandorfy C. *J. Am. Chem. Soc.* 1987; **109**: 1302.
29. Frisch MJ, Trucks GW, Schlegel HB, Gill PMW, Johnson BG, Robb MA, Cheeseman JR, Keith T, Petersson GA, Montgomery JA, Raghavachari K, Al-Laham MA, Zakrzewski VG, Ortiz JV, Foresman JB, Cioslowski J, Stefanov BB, Nanayakkara A, Challacombe M, Peng CY, Ayala PY, Chen W, Wong MW, Andres JL, Replogle ES, Gomperts R, Martin RL, Fox DJ, Binkley JS, Defrees DJ, Baker J, Stewart JP, Head-Gordon M, Gonzalez C, Pople JA. *Gaussian 94 Revision E. 1* Gaussian, Inc.: Pittsburgh, PA, 1995.